

# Observation of accelerating parabolic beams

Jeffrey A. Davis,<sup>1</sup> Mark J. Mitry,<sup>1</sup> Miguel A. Bandres,<sup>2</sup>  
and Don M. Cottrell<sup>1</sup>

<sup>1</sup>San Diego State University, Department of Physics, San Diego, CA 92182-1233

<sup>2</sup>California Institute of Technology, Pasadena, CA 91125

\*Corresponding author: jdavis@sciences.sdsu.edu

**Abstract:** We report the first observation of accelerating parabolic beams. These accelerating parabolic beams are similar to the Airy beams because they exhibit the unusual ability to remain diffraction-free while having a quadratic transverse shift during propagation. The amplitude and phase masks required to generate these beams are encoded onto a single liquid crystal display. Experimental results agree well with theory.

© 2008 Optical Society of America

OCIS codes: 050.1970, 100.5090, 140.3300, 230.6120.

---

## References and links

1. G. A. Siviloglou and D. N. Christodoulides, "Accelerating finite energy Airy beams," *Opt. Lett.* **32**, 979–981 (2007).
2. G. A. Siviloglou, J. Broky, A. Dogariu, and D. N. Christodoulides, "Observation of accelerating Airy beams," *Physical Review Letters* **99**, 213901 (2007).
3. I. M. Besieris and A. M. Shaarawi, "A note on an accelerating finite energy Airy beam," *Opt. Lett.* **32**, 2447–2449 (2007).
4. G. A. Siviloglou, J. Broky, A. Dogariu, and D. N. Christodoulides, "Ballistic dynamics of Airy beams," *Opt. Lett.* **33**, 207–209 (2008).
5. M. V. Berry and N. L. Balazs, "Nonspreading wave packets," *American Journal of Physics* **47**, 264–267 (1979).
6. M. A. Bandres, "Accelerating parabolic beams," *Opt. Lett.*, doc. ID 96139 (posted 20 June 2008, in press).
7. M. A. Bandres and J. C. Gutiérrez-Vega, "Airy-Gauss beams and their transformation by paraxial optical systems," *Opt. Express* **15**, 16719–16728 (2007).
8. K. Banerjee, S. P. Bhatnagar, V. Choudhry, and S. S. Kanwal, "The anharmonic oscillator," *Proceedings of the Royal Society of London. Series A, Mathematical and Physical Sciences* **360**, 575–586 (1978).
9. J. A. Davis, D. M. Cottrell, J. Campos, M. J. Yzuel, and I. Moreno, "Encoding amplitude information onto phase-only filters," *Appl. Opt.* **38**, 5004–5013 (1999).
10. J. B. Bentley, J. A. Davis, M. A. Bandres, and J. C. Gutiérrez-Vega, "Generation of helical Ince-Gaussian beams with a liquid-crystal display," *Opt. Lett.* **31**, 649–651 (2006).
11. J. A. Davis, C. S. Tuvey, O. López-Coronado, J. Campos, M. J. Yzuel, and C. Iemmi, "Tailoring the depth of focus for optical imaging systems using a Fourier transform approach," *Opt. Lett.* **32**, 844–846 (2007).
12. J. A. Davis, P. Tsai, D. M. Cottrell, T. Sonehara, and J. Amako, "Transmission variations in liquid crystal spatial light modulators caused by interference and diffraction effects," *Optical Engineering* **38**, 1051–1057 (1999).

---

## 1. Introduction

Recently Siviloglou et al. [1, 2, 4, 3] theoretically and experimentally demonstrated the existence of the accelerating Airy beams. These are finite-energy solutions to the paraxial wave equation that have the unusual ability to remain almost diffraction-free while having a quadratic transverse shift during propagation over long distances. These Airy beams are exponentially decaying versions of the pure Airy beams studied by Berry and Balazs [5] in 1979. While the

pure Airy beams are perfectly diffraction-less and have a quadratic transverse shift during propagation, they cannot be physically realizable because they have infinite energy. The Airy beams have finite-energy and retain these unusual properties over long distances. Recently, Bandres [6] introduced the accelerating parabolic beams that are also exact solutions of the two-dimensional paraxial wave equation. These beams have the same unusual properties as the Airy beams, but have an inherent parabolic geometry. In addition, these beams are more localized compared with the Airy beams (i.e., pure accelerating parabolic beams decay as  $x^{-1/2}$  while pure Airy beams as  $x^{-1/4}$  as  $x \rightarrow -\infty$ ) and might be more suited for practical applications.

The accelerating Airy beams have been receiving a great deal of attention because they appear to propagate in curved line. Actually this claim must be viewed with a great deal of caution. These beams exhibit a distance-dependent diffraction phenomenon where the interference maximum propagates without diffraction in a parabolic curved path. However the center of mass of the beams remains constant during propagation as expected from geometric optics [3, 4, 7].

In this work, we report the first observation of accelerating parabolic beams [6]. The accelerating parabolic beams were generated by encoding both the amplitude and phase of the Fourier transform onto a single liquid crystal display (LCD). Our experiments demonstrate that the accelerating parabolic beams can resist diffraction and experience a quadratic transverse translation during propagation over long distances.

## 2. Accelerating parabolic beams

The finite-energy accelerating parabolic beams [6] are given by

$$\phi_n(\eta, \xi, z) = e^{i(z/2k\kappa^2 - ia)(\eta^2 - \xi^2)/2} e^{i(z/2k\kappa^2 - ia)^3/3} \Theta_n(\eta) \Theta_n(i\xi), \quad (1)$$

where  $(\eta, \xi)$  are parabolic coordinates defined as

$$\left(x/\kappa - (z/2k\kappa^2)^2 + iaz/k\kappa^2, y/\kappa\right) = (\eta^2/2 - \xi^2/2, \eta\xi). \quad (2)$$

Here,  $\kappa$  is a transverse scale and  $k$  is the wave number. The functions  $\Theta_n(\eta)$ , where  $n = 0, 1, 2, \dots$ , correspond to square integrable eigensolutions of the quartic oscillator equation [8] and are depicted in Fig. 1(b). These functions are orthogonal, have  $n$  zeros and definite parity given by the parity of  $n$ . At  $z = 0$  the parameter  $a$  controls the exponential aperture function,  $\exp(ax/\kappa)$ , that ensures the containment of the accelerating parabolic beams. Therefore for finite-energy beams it is necessary that  $\text{Re}(a) > 0$ .

For  $a \ll 1$  the accelerating parabolic beams have a quasidiffraction-less behavior over long distances that increase as  $a$  decreases. The case  $a = 0$  corresponds to the pure accelerating parabolic beams that are perfectly diffraction-free but have infinite energy. From Eq. (2) we can see that during propagation the accelerating parabolic beams exhibit a transverse shift given by

$$x_s = \frac{1}{\kappa^3} \left(\frac{z}{2k}\right)^2. \quad (3)$$

It is difficult to experimentally create these beams because their width is small compared with the pixel sizes of spatial light modulators. Consequently, it is easier to generate the Fourier transforms of these beams and then optically create the desired beam in the focal plane of a lens. The Fourier spectrum of the finite-energy accelerating parabolic beams at the plane  $z = 0$  is given by [6]

$$\begin{aligned} \mathcal{F}[\phi_n](k_x, k_y) &\propto \exp\left[i\kappa^3(k_x^3/3 - a^2k_x/\kappa^2 + k_xk_y^2)\right] \\ &\times \left[\exp(-a\kappa^2(k_x^2 + k_y^2)) \Theta_n(\sqrt{2}k_y\kappa)\right]. \end{aligned} \quad (4)$$

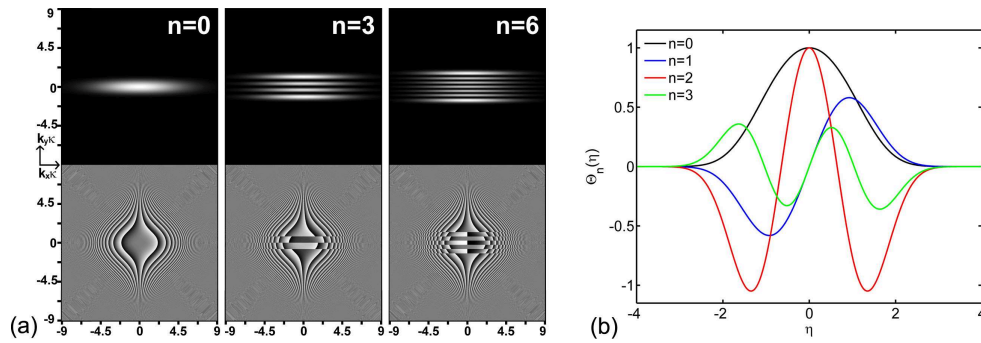


Fig. 1. (a) Theoretical intensity (top row) and phase (bottom row) of the Fourier spectrum of several accelerating parabolic beams with  $n = \{0, 3, 6\}$  and  $a = 0.02$ . (b) Few quartic oscillator eigenfunctions.

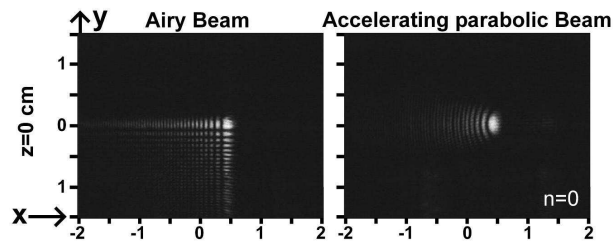


Fig. 2. Experimental results comparing the Airy and parabolic beams with  $n = 0$ ,  $a = 0.02$  and  $\kappa = 68.5 \mu\text{m}$ .

where  $(k_x, k_y)$  are the spatial frequency coordinates. The parameter  $\kappa$  controls the cubic phase that characterizes the Fourier spectrum as well as the Gaussian amplitude factor. Note that this parameter also controls the transverse shift as seen in Eq. (3).

Figure 1(a) compares the theoretical patterns for the intensity (top row) and phase (bottom row) of the Fourier spectrum for the cases of  $n = \{0, 3, 6\}$  with  $a = 0.02$ . There are two critical differences between the Fourier spectrum of the accelerating parabolic beams and the two-dimensional Airy beams. First, the phase patterns are much more complicated for large values of  $n$ . More importantly, the amplitude modulation is not a simple Gaussian as with the Airy beams. Not only it is not circularly symmetric, but there is an extra modulation in the  $k_y$ -axis given by  $\Theta_n(\sqrt{2}k_y\kappa)$ . The Gaussian factor  $\exp[-a\kappa^3(k_x^2 + k_y^2)]$  in the Fourier spectrum assures that the beam carries finite energy if  $\text{Re}(a) > 0$ .

### 3. Experiment

Accelerated Airy beams were experimentally generated [2, 4] using a phase-only LCD to encode the phase of the Fourier spectrum of the desired Airy beam. The necessary amplitude distribution is a simple two-dimensional Gaussian function that was obtained by illuminating the LCD with a Gaussian beam whose diameter had been carefully prepared. They then performed the optical Fourier transform in the focal plane of an external lens. This approach is not feasible with the accelerating parabolic beams because the amplitude distributions of their Fourier spectra are more complicated as mentioned above. Therefore another approach must be used to encode the amplitude and phase distributions.

In this work, we generate the accelerating parabolic beams by combining both the ampli-

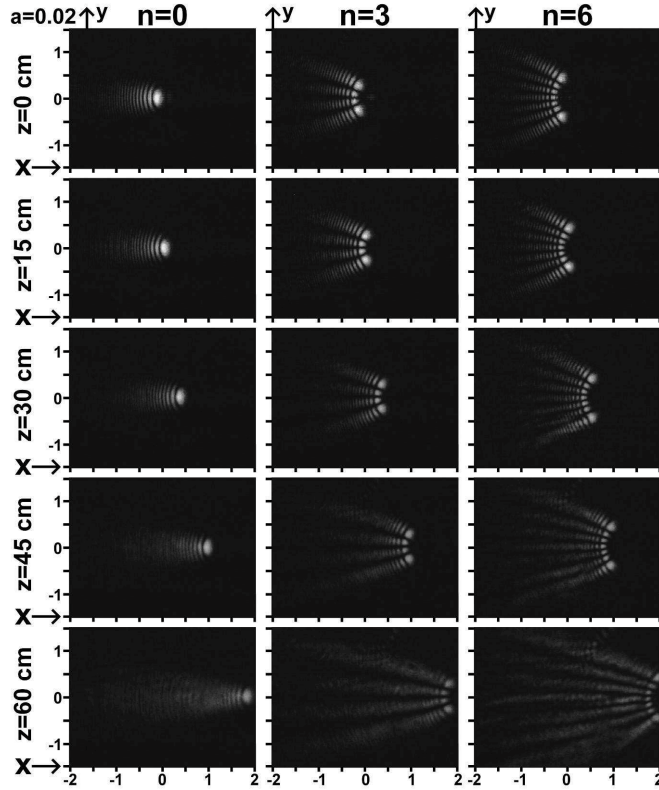


Fig. 3. Experimental results for accelerating parabolic beams with  $n = \{0, 3, 6\}$ ,  $a = 0.02$  and  $\kappa = 68.5 \mu\text{m}$  at several transverse  $z$ -planes.

tude and phase patterns onto a single LCD using a previously reported technique [9, 10, 11]. We begin with the Fourier spectrum of the desired accelerating parabolic beam function having magnitude  $M_p(x, y)$  and phase  $\phi_p(x, y)$  and written as  $M_p(x, y)\exp[i\phi_p(x, y)]$ . In this approach, we combine the phase pattern with a vertically oriented linear phase grating  $\phi_G(y) = 2\pi y/d$  with period  $d$  as  $M_p(x, y)\exp[i\phi_p(x, y) + i\phi_G(y)]$ . The total phase is the sum of the parabolic phase term with the grating phase. Amplitude information is then encoded by spatially modulating the phase pattern with the amplitude portion of the desired pattern [9, 10, 11],  $\exp\{iM'_p(x, y)[\phi_p(x, y) + \phi_G(y)]\}$ . The intensity that is diffracted into the first order varies spatially and reproduces the desired amplitude and phase distribution. There is a slight distortion that is corrected by modifying the amplitude term  $M'_p(x, y)$  as described in Ref. [9]. Here the total phase is defined  $\phi = \phi_p(x, y) + \phi_G(y)$  in the range  $[-\pi, \pi]$  while the amplitude is defined in the range  $[0 \leq M'_p(x, y) \leq 1]$ . The zero order diffraction produces an undesired term that can be spatially filtered.

In our experiments, linearly polarized light from an Argon laser is spatially filtered, expanded, and collimated. The optical elements are encoded onto a parallel-aligned nematic liquid crystal display (LCD) manufactured by Seiko Epson with  $640 \times 480$  pixels with pixel spacing of  $\Delta = 42 \mu\text{m}$  [12]. Each pixel acts as an electrically controllable phase plate where the total phase shift exceeds  $2\pi$  radians as a function of gray level at the Argon laser wavelength of 514.5 nm. The linear phase grating period  $d$  was 8 pixels  $\approx 328 \mu\text{m}$ . The Fourier transform of the mask was formed in the focal plane of a 1-meter lens to create the parabolic beam. As in

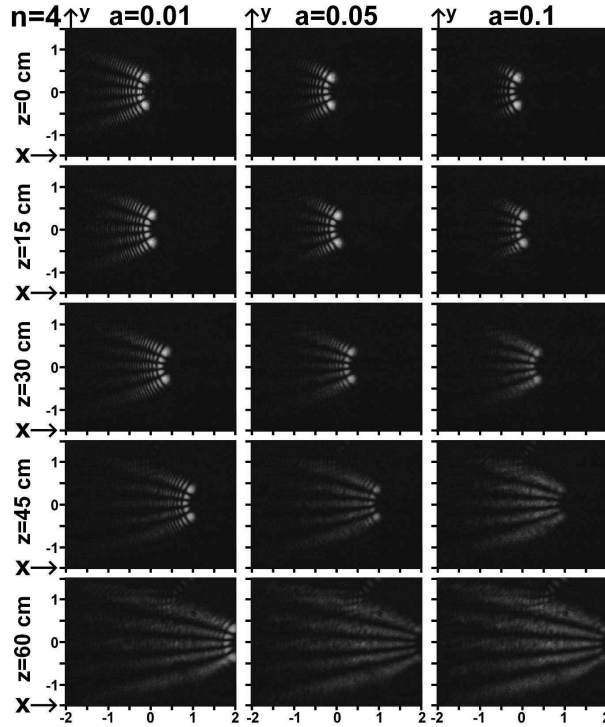


Fig. 4. Experimental results for accelerating parabolic beams with  $n = 4$ ,  $a = \{0.01, 0.05, 0.1\}$  and  $\kappa = 68.5 \mu\text{m}$  at several transverse  $z$ -planes.

Ref. [4], the LCD is placed in the front focal plane of the Fourier transform lens and the Fourier transform is formed in the back focal plane. It is possible to give an initial launch angle [4] to the accelerating parabolic beams by translating the center of the mask pattern by  $m$  pixels relative to the center of the LCD. The launch angle is related to this linear shift  $\delta = m\Delta$  by  $\theta = \delta/f$  where  $f$  is the focal length of the Fourier lens. We found this to be simpler than moving the transverse position of the Fourier lens [4]. Consequently, Eq. (3) for the transverse position of the beam is given by

$$x_s = \theta z + \frac{1}{\kappa^3} \left( \frac{z}{2k} \right)^2. \quad (5)$$

As stated earlier, our approach for encoding amplitude and phase information also generates a strong zero-order beam that was spatially filtered. The output was then recorded with a CCD camera. To magnify the image, we mounted a  $10\times$  microscope objective at a fixed distance in the front of the CCD camera [11]. By translating this assembly, we imaged various locations along the axial.

Figure 2 compares experimental results for the two-dimensional Airy beam and the parabolic beams with  $n = 0$  and where  $\kappa = 68.5 \mu\text{m}$  for both beams.

Figure 3 shows experimental results for different accelerating parabolic beams with  $n = \{0, 3, 6\}$ ,  $a = 0.02$  and  $\kappa = 68.5 \mu\text{m}$ , at propagation distances of  $z = \{0, 15, 30, 45, 60\}$  cm. The width of the image plane corresponds to  $\approx 4$  mm. As expected, the beams remain almost diffraction free for  $\approx 45$  cm and have a transverse quadratic right shift during propagation. The direction of the transverse shift can be reversed using the complex conjugate of the phase mask. The theoretical behavior is in good agreement with the experimental results and therefore is not

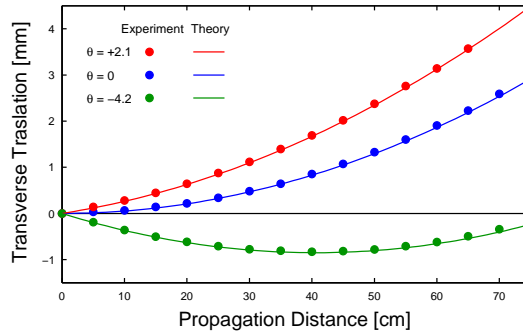


Fig. 5. Transverse deflection of an accelerating parabolic beam with  $n = 0$ ,  $a = 0.01$  and  $\kappa = 68.5 \mu\text{m}$  as a function of the propagation distance for launch angles of  $\theta = 0, +2.1, -4.2$  mrad.

shown.

Next we examine the effects of changing the parameter  $a$  of the beams. In Fig. 4 we show the experimental results for the propagation of the accelerating parabolic beams with  $n = 4$ ,  $a = \{0.01, 0.05, 0.1\}$  and  $\kappa = 68.5 \mu\text{m}$ , at propagation distances  $z = \{0, 15, 30, 45, 60\}$  cm. These experimental results show clearly that, as the parameter  $a$  decreases, the beams propagate almost diffraction-free over longer distances. For example the beams with  $a = \{0.01, 0.05, 0.1\}$  start diffracting significantly at  $z \approx \{60, 45, 30\}$  cm, respectively, as can be seen from Fig. 4.

Figure 5 shows experimental results for the quadratic transverse translation of the  $n = 0$  accelerating parabolic beam with  $a = 0.01$  and  $\kappa = 68.5 \mu\text{m}$  from  $z = 0$  to 70 cm. We show three curves with different initial launch angles of velocities using values of  $\theta = 0, +2.1, -4.2$  mrad.

To obtain an accurate measurement of the transverse translation of the beams, we compare the transverse deflection using the accelerating parabolic phase mask with the opposite deflection using the complex conjugate of the phase mask. Using one mask, we adjusted the transverse position of the camera until the beam was at one edge. We then applied the conjugate mask and moved the camera until the beam was again at the edge of the camera. The experimental accuracy of this technique was quite good at about  $75 \mu\text{m}$ . The data fits the quadratic dependence on propagation distance from Eq. (5) using the parameter  $\kappa_{exp} = 68.6 \mu\text{m}$  in excellent agreement with the theoretical value. Beams with the same parameters,  $\kappa$  and  $a$ , but different orders,  $n$ , propagate in exactly the same way and therefore they are not shown.

#### 4. Conclusion

In conclusion, we have reported the first observation of accelerating parabolic beams. As demonstrated in our experiments, the finite-energy accelerating parabolic beams exhibit the unusual ability to remain almost diffraction-free while having a quadratic transverse shift during propagation over long distances. Our experimental results agree with theory. These accelerating parabolic beams are more tightly concentrated and have lower sidelobes compared with the Airy beams. Consequently they might be more useful for practical applications as trapping.

#### Acknowledgments

J. A. Davis would like to thank Tomio Sonehara of Seiko Epson Corporation for the use of the LCD and Mark Hatay for helping with the laboratory. M. A. Bandres acknowledges support from the Secretaría de Educación Pública de México.